NeuroImage: Clinical 12 (2016) 796–805

Contents lists available at ScienceDirect

NeuroImage: Clinical

journal homepage: www.elsevier.com/locate/ynicl

Functional connectivity in cortico-subcortical brain networks underlying reward processing in attention-deficit/hyperactivity disorder

Marianne Oldehinkel[a,b,*], Christian F. Beckmann[a,b,c], Barbara Franke[b,d], Catharina A. Hartman[e], Pieter J. Hoekstra[e], Jaap Oosterlaan[f], Dirk Heslenfeld[f], Jan K. Buitelaar[a,b,g,1], Maarten Mennes[b,1]

[a] Department of Cognitive Neuroscience, Radboud University Medical Center, Nijmegen, The Netherlands
[b] Donders Institute for Brain, Cognition and Behavior, Radboud University, Nijmegen, The Netherlands
[c] Centre for Functional MRI of the Brain (FMRIB), University of Oxford, Oxford, United Kingdom
[d] Radboud University Medical Center, Departments of Human Genetics and Psychiatry, Nijmegen, The Netherlands
[e] University of Groningen, University Medical Center Groningen, Department of Psychiatry, Groningen, The Netherlands
[f] Vrije Universiteit Amsterdam, Clinical Neuropsychology Section, Amsterdam, The Netherlands
[g] Karakter Child and Adolescent Psychiatry University Centre, Nijmegen, The Netherlands

ARTICLE INFO

Article history:
Received 20 July 2016
Received in revised form 18 September 2016
Accepted 7 October 2016
Available online 8 October 2016

Keywords:
ADHD
Reward
Resting-state fMRI
Functional parcellation
Functional connectivity
Default mode network
Fronto-parietal network

ABSTRACT

Background: Many patients with attention-deficit/hyperactivity disorder (ADHD) display aberrant reward-related behavior. Task-based fMRI studies have related atypical reward processing in ADHD to altered BOLD activity in regions underlying reward processing such as ventral striatum and orbitofrontal cortex. However, it remains unclear whether the observed effects are region-specific or related to changes in functional connectivity of networks supporting reward processing. Here we use resting-state fMRI to comprehensively delineate the functional connectivity architecture underlying aberrant reward processing in ADHD.

Methods: We assessed resting-state functional connectivity of four networks that support reward processing. These networks showed high spatial overlap with the default mode, fronto-parietal, lateral visual, and salience networks, yet only activity within the salience network was effectively sensitive to reward value. We parcelled these networks into their functional cortical and subcortical subregions and obtained functional connectivity matrices by computing Pearson correlations between the regional time series. We compared functional connectivity within each of the four networks between participants with ADHD and controls, and related functional connectivity to dimensional ADHD symptom scores across all participants ($N = 444$; age range: 8.5–30.5; mean age: 17.7).

Results: We did not observe significant ADHD-related alterations in functional connectivity of the salience network, which included key reward regions. Instead, levels of inattention symptoms modulated functional connectivity of the default-mode and fronto-parietal networks, which supported general task processing.

Conclusions: The present study does not corroborate previous childhood evidence for functional connectivity alterations between key reward processing regions in adolescents and young adults with ADHD. Our findings could point to developmental normalization or indicate that reward-processing deficits result from functional connectivity alterations in general task-related networks.

1. Introduction

Aberrant reward processing is considered to be a key feature of attention-deficit/hyperactivity disorder (ADHD; Luman et al. 2005; Sonuga-Barke 2005). Compared to healthy controls, both youth and adults with ADHD show a preference for small immediate rewards over larger delayed rewards (Bitsakou et al. 2009; Marco et al. 2009), make more risky decisions to obtain rewards (Groen et al. 2013), and are more sensitive to the positive effects of rewards while performing cognitive tasks (Luman et al. 2010; Uebel et al. 2010).

Several task-based functional magnetic resonance imaging (fMRI) studies have invested in mapping the neurobiological basis of reward processing in the brain using a variety of reward-probing paradigms. Key structures identified include the dopaminergic midbrain, ventral striatum (including the nucleus accumbens (NAcc)), anterior cingulate cortex (ACC), and orbitofrontal cortex (OFC; Haber and Knutson 2010). Furthermore, several other brain regions such as dorsolateral prefrontal cortex (DLFPC), insula, cerebellum, thalamus, hippocampus, and amygdala, are thought to be important in regulating the reward network (Haber and Knutson 2010; Liu et al. 2011). In the context of

* Corresponding author at: Kapittelweg 29, 6525 EN Nijmegen, The Netherlands.
E-mail address: m.oldehinkel@donders.ru.nl (M. Oldehinkel).
[1] Shared last authorship.

http://dx.doi.org/10.1016/j.nicl.2016.10.006

both childhood and adulthood ADHD, studies have shown decreased BOLD responses in ventral striatum, precuneus, posterior cingulate cortex (PCC) and medial prefrontal cortex (PFC) during reward anticipation (Chantiluke et al. 2014; Hauser et al. 2014; Plichta and Scheres 2014; Rubia et al. 2009; Scheres et al. 2007), increased BOLD responses in ACC and cerebellum during reward anticipation (von Rhein et al. 2015), as well as increased BOLD responses in OFC and occipital cortex during reward receipt (von Rhein et al. 2015).

As neuroimaging is shifting its focus from localizing functions in individual regions to investigating the integration of functionally related areas into larger networks, it becomes increasingly clear that ADHD is not related to dysfunction in isolated brain areas (Oldehinkel et al. 2013). Accordingly, dysfunctional integration within and between reward-related regions may underlie deficient reward processing in ADHD. Initial evidence comes from studies that used resting-state fMRI (R-fMRI) to investigate functional integration within the reward-network in children with ADHD. One of these studies reported *decreased* functional connectivity of ventral striatum with OFC, hippocampus, and anterior PFC in ADHD (Posner et al. 2013; age range: 7–12 years, 22 ADHD participants; 20 controls). Yet, others revealed *increased* functional connectivity of OFC with NAcc and ACC (Tomasi and Volkow 2012; mean age 10.8 ± 1.8 SD; 247 ADHD participants, 309 controls), and of NAcc with ventromedial and anterior PFC in ADHD (Costa Dias et al. 2012; age range: 7–12 years; 35 ADHD participants, 64 controls). Furthermore, these three studies were all conducted in children, while ADHD is known to persist into adolescence and adulthood in many patients (Faraone et al. 2006).

Accordingly, building on these initial studies, we aimed to comprehensively delineate the functional neural architecture underlying aberrant reward processing in ADHD. To this end, we investigated ADHD-related changes in resting-state functional connectivity of networks that support reward processing using a large ADHD cohort ($N = 444$) with a wide age range (8.5–30.5 years). We made use of large-scale functional networks derived during reward processing (von Rhein et al., in revision), thereby extending our focus beyond the reward regions typically identified using highly specific task contrasts. To be able to investigate connectivity within each network, we identified the functional cortical subregions within each network and also assessed each network's cortico-subcortical integration by examining its connectivity with cerebellum, thalamus, and striatum. Next, using diagnostic categories as well as dimensional ADHD symptom measures, we determined the impact of ADHD on these functional connectivity patterns.

2. Material and methods

2.1. Participants

Participants in our study were part of the NeuroIMAGE cohort (von Rhein et al. 2014), consisting of families with one or more children with an ADHD diagnosis as well as control families with children without an ADHD diagnosis. Diagnosis of ADHD and comorbid disorders (including oppositional defiant disorder (ODD), conduct disorder (CD), anxiety disorders, and depression) were assessed by trained psychologists using the Schedule for Affective Disorders and Schizophrenia for School-Age Children - Present and Lifetime Version (K-SADS; Kaufman et al. 1997), complemented with Conners' ADHD questionnaires (Conners et al. 1998a; Conners et al. 1998b). Participants were diagnosed with ADHD if they displayed six or more DSM-5 ADHD symptoms on at least one domain (inattention or hyperactivity/impulsivity; five or more for participants >18 years). Participants from control families and unaffected siblings of participants with ADHD were allowed to have a maximum of two ADHD symptoms per domain. Participants not belonging to one of these groups were classified as subthreshold ADHD. Next to this categorical classification, we used ADHD symptom scores for inattention and hyperactivity/impulsivity derived from the Conners' Parent Rating Scale (CPRS-RL; Conners et al. 1998a) for our dimensional analyses. The CPRS-RL is an ADHD rating scale from which standardized T-scores ranging from 40 to 90 can be obtained. The full description of the NeuroIMAGE cohort, including inclusion criteria, diagnostic assessment, and general testing procedures can be found in von Rhein et al. (2014). Our study was approved by local ethical committees of the participating centers and conducted in compliance with the Declaration of Helsinki. Written informed consent was obtained from all participants (for participants >12 years) and their legal guardians (for participants <18 years).

For the current analysis we selected participants who completed both an anatomical and an 8-minute R-fMRI scan ($N = 507$). We excluded participants with high head-motion ($N = 47$, as determined by calculating the mean root mean square of the frame-wise displacement (RMS-FD > 0.5; Jenkinson et al. 2002) across the R-fMRI scan) and participants with insufficient brain coverage during the R-fMRI scan ($N = 16$). This procedure led to the inclusion of 444 participants in total, including participants with ADHD ($N = 169$), healthy controls ($N = 122$), unaffected siblings of participants with ADHD ($N = 89$), and participants with subthreshold ADHD ($N = 64$). The characteristics of participants included in our analyses are specified in Table 1. Out of the 169 participants with an ADHD diagnosis in our sample, 83 participants had the inattentive presentation, 17 participants had the hyperactivity-impulsive presentation and 69 participants had the combined presentation. In our analyses we chose not to investigate these subgroups separately, given the emphasis of this paper to move towards a more dimensional investigation of ADHD, which (partly) captures this heterogeneity in symptoms. In the ADHD group, 130 participants were on stimulant medication, however, all participants withheld medication starting 48 h before the day of assessment.

2.2. MRI data acquisition and preprocessing

MRI data were acquired at two locations on 1.5 Tesla scanners from Siemens (Siemens AVANTO at the Donders Institute for Brain, Cognition and Behavior in Nijmegen and Siemens SONATA at the VU University Medical Centre in Amsterdam). At both sites identical 8-channel head coils and MRI protocols were employed. Structural images were obtained using an MPRAGE sequence (TR = 2730 ms, TE = 2.95 ms, T1 = 1000 ms, voxel size = 1 × 1 × 1 mm, flip angle = 7, matrix size = 256 × 256, FOV = 256 mm, 176 slices). The R-fMRI data were acquired using a gradient echo-planar imaging sequence (TR = 1960 ms, TE = 40 ms, flip angle = 80, matrix size = 64 × 64, in-plane resolution = 3.5 mm, FOV = 224 mm, 37 axial slices, slice thickness/gap = 3.0 mm/0 mm/0.5 mm, 265 volumes). Participants were instructed to relax and keep their eyes open for the duration of the R-fMRI scan.

The R-fMRI data were preprocessed using a standard preprocessing pipeline incorporating tools from the FMRIB Software Library (FSL version 5.0.6; http://www.fmrib.ox.ac.uk/fsl). Our pipeline included removal of the first five volumes to allow for signal equilibration, primary head movement correction via realignment to the middle volume (MCFLIRT; Jenkinson et al. 2002), grand mean scaling, and spatial smoothing using a 6 mm FWHM Gaussian kernel. Next, ICA-AROMA was applied to the R-fMRI data to select and remove components that represent secondary head motion-related artifacts (Pruim et al. 2015a; Pruim et al., 2015b), followed by nuisance regression to remove signal from white matter and cerebrospinal fluid, and a high-pass filter (0.01 Hz). The R-fMRI images of each participant were co-registered to the participants' anatomical images by means of boundary-based registration implemented in FSL-FLIRT (Greve and Fischl 2009). The T1 images of each participant were registered to MNI152 standard space using 12-parameter affine transformation and refined using non-linear registration with FSL-FNIRT (10 mm warp, 2 mm resampling resolution; Jenkinson et al. 2002). Finally, we brought all R-fMRI images to MNI152 standard space by applying the concatenated R-fMRI to T1 and T1 to MNI152 transformations.

Table 1
Participant characteristics.

	Controls (C) $N = 122$		ADHD (A) $N = 169$		Test statistic		Subthreshold $N = 64$		Siblings $N = 89$	
Demographic (mean, SD)										
Age, years	17.04	2.98	17.89	3.07	$t(289) = 2.36^{*}$	A > C	18.37	3.32	17.63	4.12
IQ[a]	106.6	13.9	96.08	15.1	$t(289) = -6.08^{**}$	A < C	100.7	12.9	102.1	14.9
Medication use, years	–	–	2.41	3.12	–	–	1.95	3.13	0.002	0.01
Motion[b]	0.125	0.09	0.140	0.10	$t(289) = 1.35$	–	0.129	0.09	0.113	0.09
Demographic (number, %)										
Sex, male	54	44.3	123	72.8	$X^2(1) = 24.18^{**}$	A > C	38	59.4	35	39.3
Scan location, *Nijmegen*	48	39.3	92	54.4	$X^2(1) = 6.65^{*}$	A > C	36	56.3	46	51.7
ODD[c]	–	–	46	27.2	–	–	8	12.5	2	2.25
CD[d]	–	–	6	3.80	–	–	–	–	–	–
Clinical (mean, SD)										
Hyperactive/impulsive symptoms[e]	46.45	5.24	69.59	14.2	$t(289) = 17.19^{**}$	A > C	54.70	11.70	47.71	6.46
Inattentive symptoms[e]	46.12	5.72	66.09	10.9	$t(289) = 18.49^{**}$	A > C	54.07	8.57	46.81	6.16
Cognitive (mean, SD)										
Reward-related speeding[f]	27.1	25.7	30.8	37.1	$t(153) = -0.74$	A = C	20.0	21.9	32.0	27.1

The test statistics only compare the ADHD (A) and control (C) group given that only these groups were included in the categorical analysis. The dimensional analyses included all participants listed in this table independent of diagnostic label $^{*}p < 0.05$, $^{**}p < 0.001$.

[a] Estimated IQ based on Wechsler Intelligence Scale for Children or Wechsler Adult Intelligence Scale–III Vocabulary and Block Design (Wechsler 2000, 2002).

[b] Motion as measured by the root mean square frame-wise displacement (RMS-FD; Jenkinson et al. 2002).

[c] Oppositional Defiant Disorder (ODD).

[d] Conduct Disorder (CD).

[e] Conners Parent Rating Scale questionnaire, standardized *T*-score (Conners et al. 1998a) Range min. 40 to max. 90 (≥63 is clinical threshold).

[f] This data was available for approximately half of our sample: Controls: $N = 64$, ADHD: $N = 91$, Subthreshold: $N = 31$, and Siblings: $N = 49$. Difference in RT (ms) between reward trials and neutral trials during the monetary incentive delay task.

2.3. Networks supporting reward processing

We examined functional connectivity in relation to four networks that were identified to support reward processing during performance of a monetary incentive delay (MID) task (von Rhein et al. in revision; for a description of the specific task effects see von Rhein et al. 2015). In short, von Rhein et al. derived these four networks through a meta-independent component analysis (meta-ICA) across typical first-level

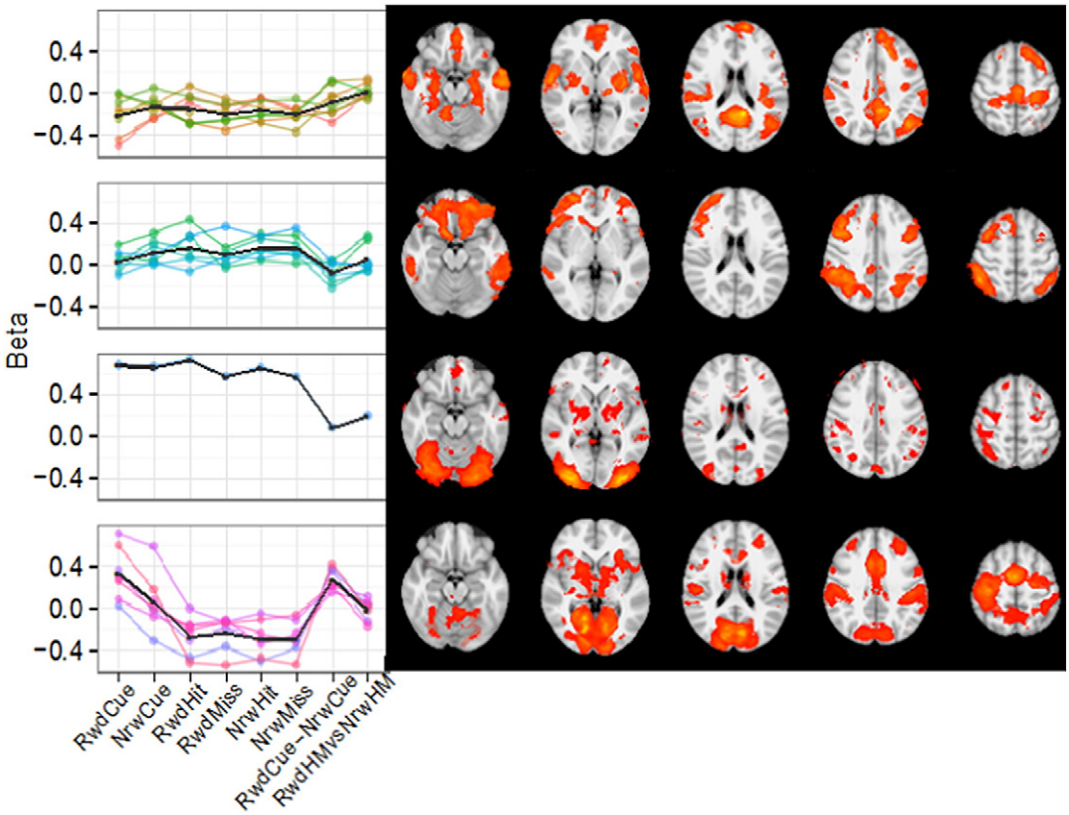

Fig. 1. K-means clustered profiles and spatial maps of non-noise components. These components were obtained by applying a meta-ICA analysis to fMRI data of 60 control participants performing the monetary incentive delay task (MID). Black lines in the task condition profiles indicate mean for each cluster. Spatial maps of independent components are averaged across cluster and thresholded ($Z > 2.3$). Major networks that correspond with the different clusters are: 1) default mode network, 2) fronto-parietal network, 3) lateral visual network, and 4) salience network. Abbreviations: RwdCue = reward cue, NrwCue = no-reward cue, RwdHit = reward hit, RwdMiss = reward miss, NrwHit = no-reward hit, NrwMiss = no-reward miss, RwdCue-NrwCue = reward cue versus no-reward cue (reward anticipation), RwdHMvsNrwHM = reward hit and miss versus no-reward hit and miss (reward outcome). For details see von Rhein et al. in revision and our Supplementary material.

MID activation maps of 60 control participants (see von Rhein et al. (in revision) or the Supplementary material for a detailed description of this analysis). The meta-ICA approach resulted in 23 non-noise, whole-brain independent components (see Supplementary Fig. S1) that were further clustered based on their association with the specific conditions of the reward task (see Supplementary Fig. S2), resulting in four average task condition profiles and four corresponding clusters of components (i.e., networks) relevant for reward processing. The spatial maps for these networks are shown in Fig. 1.

The obtained functional networks presented in Fig. 1 showed high spatial similarity with known resting-state networks. The first three clusters respectively resembled the default mode network (DMN; yet including insular and motor cortex), the fronto-parietal network, and the lateral visual network. These clusters showed average loadings on nearly all task aspects, indicating that these networks contributed to the general execution of the MID task, but were not specific to processing reward. In contrast, the fourth cluster was specifically related to reward processing as it had strong loadings for reward cues, reward anticipation, and reward outcome. This cluster showed high spatial similarity with the salience network, including core regions typically implicated in reward processing, such as NAcc and ACC (Haber and Knutson 2010).

2.4. Delineation of functional cortical and subcortical regions within the large-scale networks

To investigate the functional connectivity architecture of the identified networks we set out to delineate functional subregions within each of the four networks obtained above. First, we parcelled the cortical regions within each network by applying a novel, top-down functional parcellation technique called Instantaneous Correlation Parcellation (ICP; van Oort et al. in preparation). ICP divides a larger predefined network into subregions based on subtle differences in its voxels' time series. A detailed description of the ICP strategy is provided in the Supplementary material. For each of the four networks we generated an independent parcellation using R-fMRI data from 100 subjects of the publically available Human Connectome Project dataset (HCP; Smith et al. 2013; see the Supplementary material for a detailed description).

Next, we investigated cortico-subcortical connectivity for each network by segregating structural masks of striatum, thalamus, and cerebellum based on functional connectivity strength with the cortical regions obtained for each network. To this end, we calculated partial correlations between every subcortical voxel and the ICP-based cortical regions within each network (as implemented in FSL sbca; O'Reilly et al. 2010). This was done for each of 100 participants in a second sample of the HCP dataset (subject IDs are provided in the Supplementary material). The obtained participant-level partial correlation maps were converted to *z*-stat maps using the Fisher's r-to-*z* transformation and entered in a group-level analysis using FSL randomize (5000 permutations; Winkler et al. 2014). This resulted in group-level maps indicating the connectivity strength of each subcortical voxel with each ICP-based cortical region for every network. We then used a 'winner-takes-all' approach assigning each voxel in striatum, thalamus, and cerebellum to the cortical region with which it showed the strongest functional connectivity. That is, we delineated regions within respectively striatum, thalamus, and cerebellum by grouping voxels that showed strongest connectivity with the same cortical region. Note, that we used a structural mask of striatum, thalamus, and cerebellum to allow full investigation of subcortical involvement in the context of ADHD, as opposed to including the subcortical regions as included in the four networks. As shown in Supplementary Fig. S7, the four networks did not fully cover subcortex.

2.5. Functional connectivity analyses

We used the cortical and subcortical regions obtained from the functional parcellation of each network as masks to extract R-fMRI timeseries for the current sample (i.e., participants of the NeuroIMAGE cohort). These timeseries were extracted from each participant's R-fMRI data after transformation to MNI152 2 mm standard space. First we extracted timeseries for all voxels within each mask and applied a singular value decomposition. We then selected the first eigenvariate and used the associated time series as the time series that most accurately represented the respective cortical or subcortical region.

We computed Pearson and partial correlations between all the extracted time series within each network for every participant. All following steps were conducted for both Pearson and partial correlations. The obtained correlations were transformed into normally distributed values using Fisher's r-to-*z* transformation. We corrected for potential confounding effects of age, sex, scan location, and ODD/CD comorbidity by means of conducting an ordinary least squares (OLS) regression for every correlation. Next, we conducted categorical analyses in which we compared functional connectivity within the four networks between the ADHD group ($N = 169$) and control group ($N = 122$), as well as dimensional analyses in which we investigated the relationship between functional connectivity and ADHD symptom measures across all 444 participants (i.e., ADHD participants, controls, unaffected siblings of ADHD participants, and subthreshold ADHD cases). More specifically, categorical ADHD versus control group differences in the residual correlation strength were tested for significance using permutation testing with 10,000 permutations for every pair of regions. We obtained *p*-values by calculating the fraction of permuted samples that yielded a difference between the ADHD and control group larger than the observed difference. Similarly, in the dimensional analyses we investigated the relationship of functional connectivity between every pair of regions and CPRS inattention and hyperactivity/impulsivity scores across all participants. We likewise obtained p-values by calculating the fraction of permuted samples that yielded a correlation between symptom scores and functional connectivity higher than the observed correlation. Finally, for both the categorical and dimensional analyses we corrected for multiple comparisons within each network by applying a False Discovery Rate (FDR) correction ($p < 0.05$) to the obtained p-values.

In addition, we assessed functional connectivity in subnetworks within each of the four larger networks. These subnetworks were based on the results from the 'winner-takes-all' procedure, i.e., subnetworks were formed by grouping every cortical subregion with the subregions in respectively striatum, thalamus, and cerebellum with which it showed the highest connectivity. To assess functional connectivity within these subnetworks we computed the average value across Pearson or partial correlations between all pairs of regions within each subnetwork. The same procedure as described above was followed to convert the obtained average Pearson and partial correlations within each subnetwork into normally distributed values, to correct for confounding effects, and to test categorical and dimensional ADHD-related effects for significance. Given the limited number of comparisons ($N = 4$; see results) we implemented correction for multiple comparisons using Bonferroni (i.e., 0.05 divided by the number of subnetworks within each larger network) instead of FDR.

For functional connections showing significant associations with ADHD in the categorical or dimensional analyses, we conducted post-hoc analyses examining whether these effects were associated with reward-related behavior. To this end, we correlated functional connectivity with reward-related speeding (available for 228 participants) across participants, while correcting for effects of age, sex, scan location, and ODD/CD comorbidity. Reward-related speeding was calculated as the difference in reaction time between rewarded trials and neutral trials during the MID task (as described in von Rhein et al. 2015). Finally, to rule out that findings were driven by scan location, sex, age, IQ, medication history, or ODD/CD comorbidity, we conducted post-hoc sensitivity analyses, as described in the Supplementary material (Tables S3 and S4).

3. Results

3.1. Parcellation of networks supporting reward processing

We applied ICP to obtain parcellations of the cortex ranging from two to twenty subregions for each of the four networks supporting reward processing. For each network, the parcellation into four subregions yielded high reproducibility scores of at least 90% spatial overlap (i.e., DICE-overlap) between split-half analyses (see Supplementary Fig. S6). Accordingly, we used the cortical parcellation into four subregions for each network for further analyses. The obtained cortical regions within each network are displayed in the left panel of Fig. 2. All parcellations showed high spatial similarity between the left and right hemisphere. To summarize, the first three clusters in network 1 respectively consisted of frontal medial cortex (FMC) and frontal pole (green), precentral gyrus (brown), and insular cortex and supramarginal cortex (yellow). The fourth cluster within this network was formed by the precuneus/PCC and superior FMC (blue), which are considered key regions of the DMN. Network 2 was segregated in four cortical clusters, each consisting of spatially distinct frontal and parietal regions that displayed high left-right symmetry. Network 3 was subdivided in four cortical clusters consisting of the occipital pole (green), lateral occipital cortex and occipital fusiform gyrus (brown), and several smaller clusters in the temporal and parietal lobes (blue and yellow). Finally, network 4, which was specifically related to reward processing, was parcellated into two occipital clusters (green and blue), a cluster consisting of motor areas (brown), and a cluster including supramarginal cortex, frontal pole, insula, and cingulate cortex (yellow).

We delineated the subcortical components separately for each network, by assigning each subcortical voxel to the cortical region with which it showed the highest functional connectivity using a 'winner-takes-all' approach. The resulting network-specific subregions within striatum, thalamus, and cerebellum are shown in matching colors in the right panel of Fig. 2. High overlap was present between the obtained subcortical parcellations of the four networks, yet there were also network-specific characteristics. Overall, cerebellum, striatum, and thalamus were functionally connected with various clusters in frontal, temporal, and parietal cortices, whereas there appeared to be relatively little connectivity with occipital cortex. In accordance with the literature, the putamen, the ventral lateral nucleus (VL), ventral lateral posterior nucleus (VLP), and ventral posterior lateral nucleus (VPL) of the thalamus, and cerebellar lobules VI and VIII were strongly connected with motor and somatosensory cortices (Di Martino et al. 2008; O'Reilly et al. 2010; Zhang et al. 2010) This pattern was present across all four networks. Within the cerebellum, however, there were also clear network-specific differences. For example, whereas lobules IV, V, and IX (located medially in the cerebellum) were assigned to regions of the DMN in network 1, they were assigned to the primary visual cortex in network 4.

3.2. Functional connectivity within networks supporting reward processing

We investigated functional connectivity within each network by computing Pearson and partial correlations between the timeseries extracted for all regions within the network. The resulting group-average connectivity matrices for each network are shown in Fig. 3 (ADHD and controls) and Supplementary Fig. S8 (unaffected siblings and

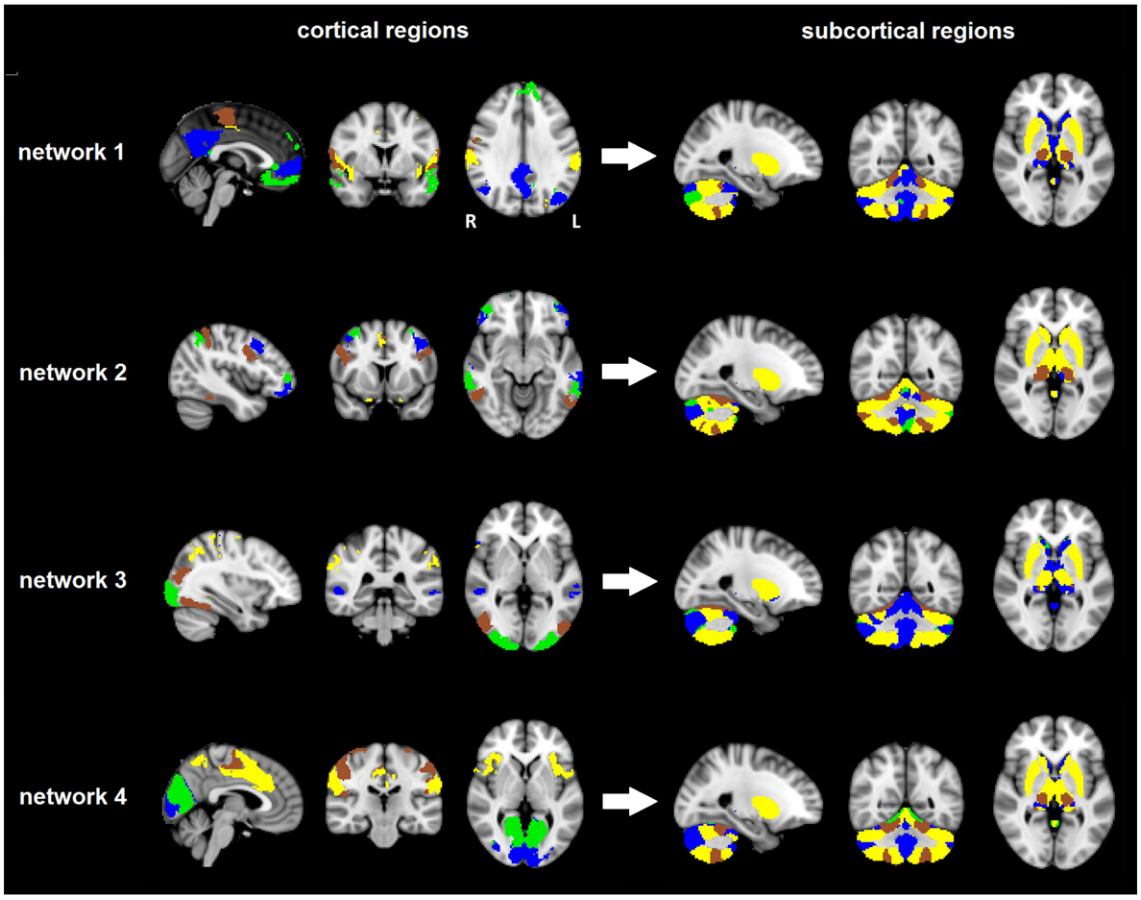

Fig. 2. The obtained cortical and subcortical subregions for each of the four networks. The four cortical subregions resulting from the ICP parcellation of each network are shown on the left side of the figure. The delineated network-specific subcortical subregions are shown on the right side of the figure in matching colors (i.e., the subcortical regions are displayed in the same color as the cortical region with which they exhibited the strongest functional connectivity).

subthreshold cases). Pearson correlations are represented in the upper right triangle and partial correlations in the lower left triangle of each connectivity matrix. However, as can be observed in Figs. 3 and S4, nearly all partial correlations were approximating zero. Partial correlations represent the correlation between two regions after accounting for the variance they share with all other regions in the analysis. Given that in our study we focused on cortical-subcortical connections within each functional network the amount of shared variance between subregions within each network was likely high. As such, most variance, including variance representing effects of interest, is partialled out when calculating partial corrections. Accordingly, we selected the Pearson correlations for further analyses.

A pattern observed across networks 2, 3, and 4 in all diagnostic groups was that functional connectivity was relatively strong (i.e., high Pearson correlations) for intracortical and intracerebellar connections, whereas connectivity was overall lower for cortico-thalamic and

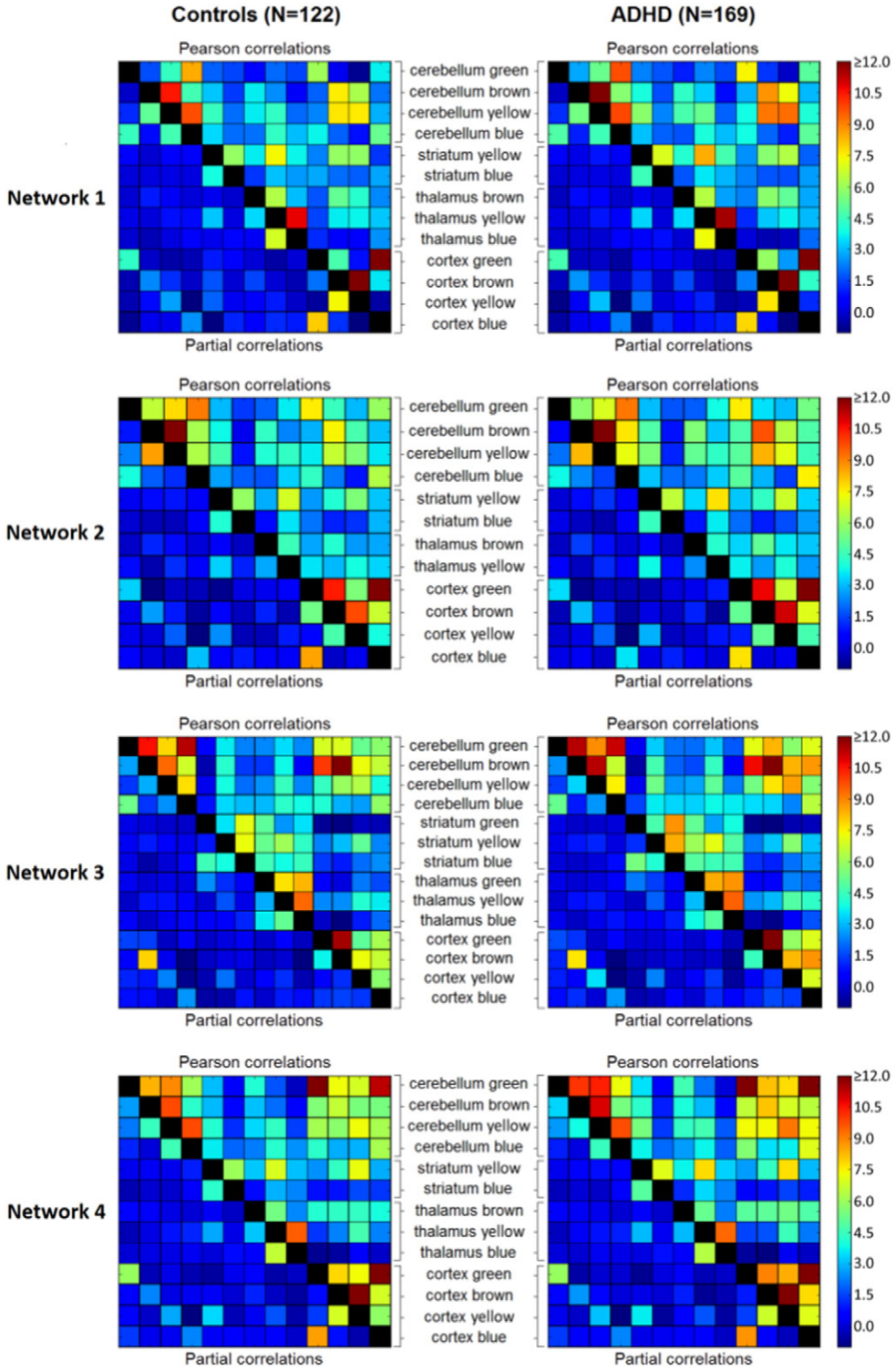

Fig. 3. Group-average connectivity matrices showing z-transformed Pearson and partial correlations between timeseries of the different subcortical and cortical subregions in the four networks. No significant differences in correlations were present between the ADHD and control group in any of the four networks. Connectivity matrices for the unaffected siblings and subthreshold ADHD participants can be found in Supplementary Fig. S8.

cortico-striatal connections. In network 1, connectivity was high for some, but not for all intracortical connections. Network 1 included components of the DMN, such as FMC (blue and green) and PCC (blue), but also other regions implicated in task-positive networks, such as precentral gyrus (brown) and insular and supramarginal cortex (yellow). In line with previous studies (Buckner et al. 2008), connectivity strength was low for functional connections between DMN and task-positive regions within network 1. Within networks 3 and 4, functional connectivity was also relatively high for most functional connections between cortical and cerebellar regions, whereas this was less evident in networks 1 and 2. Finally, unique to network 3 (showing high spatial similarity with the lateral visual network), connectivity was strong for all intra-thalamic connections. This was expected, as visual perception is known to be influenced by thalamic signaling (Pollen 1999).

3.3. ADHD-related changes in network characteristics

We investigated ADHD ($N = 169$) versus control ($N = 122$) group differences in functional connectivity between all pairs of subregions within each network by means of permutation testing (while correcting for confounding effects and multiple comparisons). These analyses did not reveal significant differences in functional connectivity between the ADHD and control group in any of the four networks.

Next, we investigated dimensional effects of ADHD across all participants ($N = 444$), including unaffected siblings and subthreshold cases, by relating participant-level CPRS inattention and hyperactivity/impulsivity symptom ratings to functional connectivity between the different subregions within the four networks (see Fig. 4). Correcting for confounding effects and multiple comparisons, we observed significant relationships between CPRS inattention scores (but not hyperactivity/impulsivity scores) and seven functional connections in network 1 (this network exhibited high spatial similarity with the DMN). Specifically, increased inattention scores were associated with increased functional connectivity between the following pairs of regions in network 1 (colors as shown in Fig. 2): cerebellum brown – cerebellum yellow, cerebellum brown – cortex green, cerebellum yellow – thalamus brown, cerebellum yellow – cortex green, thalamus brown – cortex yellow, cortex green – cortex yellow, and cortex blue – cortex yellow. The anatomical labels of these region-pairs and the statistical parameters are listed in Table 2; representations of these seven dimensional relationships can be found in Supplementary Fig. S9. Post-hoc sensitivity analyses showed that obtained functional connectivity metrics were not related to scan location, sex, age, IQ, medication history, or ODD/CD comorbidity (see Supplementary Tables S3 and S4). We did not observe significant dimensional ADHD-related effects in network 4, which included key regions typically implicated in reward processing, or in networks 2 and 3.

We also examined categorical and dimensional ADHD-related changes in the average functional connectivity within each subnetwork (i.e., regions of the same color in Fig. 2) in the four larger networks. No differences in functional connectivity were observed in the categorical analyses comparing the ADHD and control group, yet we did observe a significant effect in the dimensional analysis of network 2 (this network exhibited high spatial similarity with the fronto-parietal network). Specifically, increased inattention scores were associated with increased functional connectivity in the brown subnetwork within network 2 (Supplementary Fig. S10; $r = 0.175$, $p = 0.0013$). The subcortical regions within this subnetwork corresponded with bilateral cerebellar lobules V, VI, VIIIa, VIIIb, and IX, and bilateral thalamic VL, VLP, and VPL nuclei. The cortical regions within this subnetwork were bilateral inferior temporal gyrus, bilateral precentral gyrus, a posterior

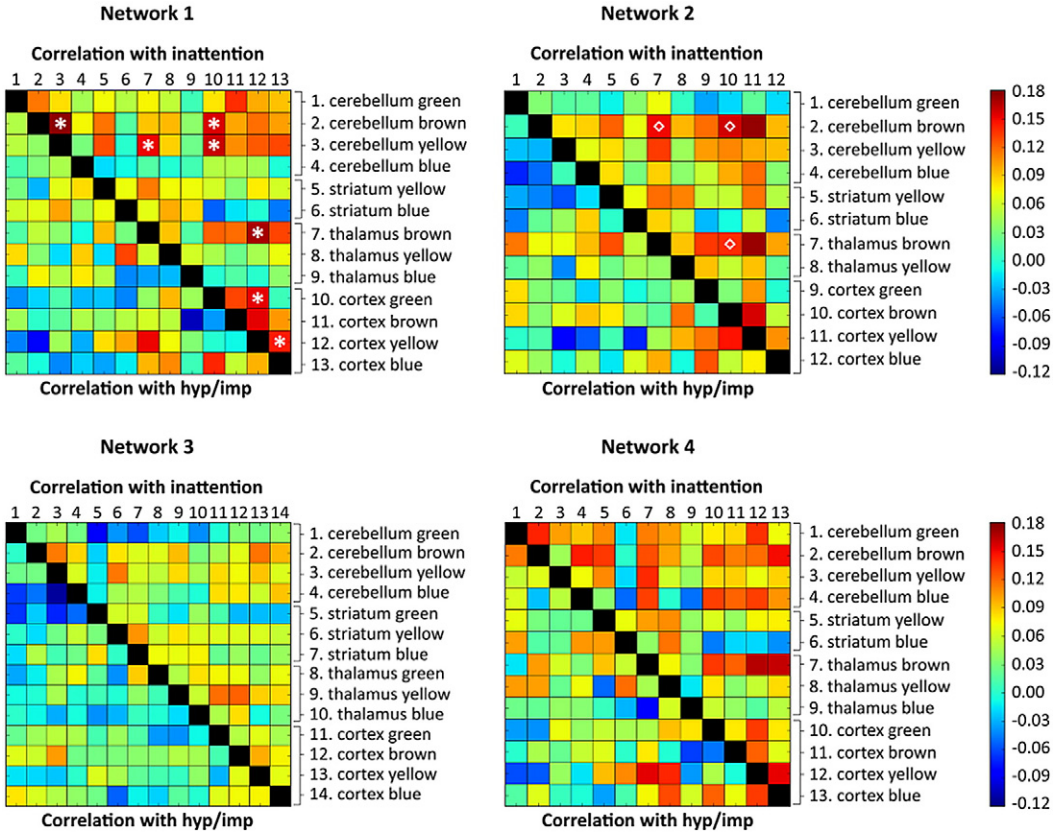

Fig. 4. Matrices indicating the correlation of inattention and hyperactivity/impulsivity (hyp/imp) symptom scores with connectivity (i.e., Pearson correlations) between the timeseries of the different subcortical and cortical subregions in the four networks across all participants ($N = 444$). Inattention and hyperactivity/impulsivity scores were based on the Conners parent rating scale (CPRS; Conners et al. 1998a). Asterisks (*) indicate significant correlations in network 1 after correction for covariates (age, sex, scan location, and comorbid ODD/CD) and multiple comparisons (FDR; $p < 0.05$). Similarly diamonds (◇) indicate significant connections of the brown subnetwork within network 2. (For interpretation of the references to color in this figure legend, the reader is referred to the web version of this article.)

Table 2
Statistical parameters of significant inattention-related increases in functional connectivity in network 1.

Functional connection	Corresponding anatomical labels*	Correlation with inattention	*P*-value based on 10,000 permutations**	FDR-corrected *p*-value
Cerebellum brown Cerebellum yellow	Lobules V/VI, VIIIa/VIIIb Lobules VI/VIIb/VIIIa/VIIIb/IX/crus1/crus2/vermis IV/VI	$r = 0.176$	$p = 0.0004$	$p = 0.0312$
Cerebellum brown Cortex green	Lobules V/VI, VIIIa/VIIIb FMC, SFG, MTG	$r = 0.156$	$p = 0.0031$	p = 0.0455
Cerebellum yellow Thalamus brown	Lobules VI/VIIb/VIIIa/VIIIb/IX/crus1/crus2/vermis IV/VI VL/VLP/VPL	$r = 0.151$	$p = 0.0035$	p = 0.0455
Cerebellum yellow Cortex green	Lobules VI/VIIb/VIIIa/VIIIb/IX/crus1/crus2/vermis IV/VI FMC, SFG, MTG	$r = 0.160$	$p = 0.0019$	p = 0.0455
Thalamus brown Cortex yellow	VL/VLP/VPL Insular cortex/PreCG, SMG	$r = 0.169$	$p = 0.0023$	p = 0.0455
Cortex green Cortex yellow	FMC, SFG, MTG Insular cortex/PCG, SMG	$r = 0.152$	$p = 0.0024$	$p = 0.0455$
Cortex blue Cortex yellow	Precuneus/PCC, ParaCG, LOC Insular cortex/PCG, SMG	$r = 0.144$	$p = 0.0044$	$p = 0.0490$

Abbreviations: FMC = fronto-medial cortex, LOC = lateral occipital cortex, MTG = middle temporal gyrus, PCC = posterior cingulate cortex, paraCG = paracingulate gyrus, PreCG = precentral gyrus, SFG = superior frontal gyrus, SMG = supramarginal gyrus, VL = ventral lateral nucleus, VLP = ventral lateral posterior nucleus, VPL = ventral posterior lateral nucleus.
* Labels based on the Cerebellar atlas (FSL), morel histological thalamic atlas (Morel 2007), and Harvard-Oxford cortical atlas.
** Corrected for confounding effects of age, sex, scan location, and comorbid ODD/CD.

cluster consisting of bilateral supramarginal gyrus, superior parietal cortex, and lateral occipital cortex, and a frontal cluster consisting of left inferior and left middle frontal gyrus. No associations between inattention or hyperactivity/impulsivity and functional connectivity were observed in the other networks. Post-hoc sensitivity analyses showed that functional connectivity in the brown subnetwork within network 2 was not related to scan location, sex, IQ, medication history, or ODD/CD comorbidity (see Supplementary Tables S3 and S4), although a significant correlation with age was observed, confirming the usefulness of adding age as a covariate in our analyses.

3.4. Relationships with reward-related behavior

Functional connectivity (i.e., Pearson correlations) for functional connections in network 1 and 2 that showed significant associations with inattentive symptoms, was not associated with reward-related speeding (network 1: all $-0.067 > r < 0.105$, $p > 0.144$; network 2: $r = 0.020$, $p = 0.757$).

4. Discussion

Although considered a key deficit in ADHD evidence for aberrant functional connectivity of reward processing areas in ADHD is heterogeneous, including inconsistencies in the specific reward-related areas reported on. Here we applied a delineation of the functional neural architecture underlying reward processing to investigate possible alterations in cortico-subcortical connectivity in ADHD. In our results, ADHD was not associated with functional connectivity in a reward specific network including the NAcc and ACC (i.e., network 4). As such, we did not replicate previous findings of aberrant functional connectivity between key reward-related brain regions in ADHD (Costa Dias et al. 2012; Posner et al. 2013; Tomasi and Volkow 2012). Yet, we did observe that functional connectivity in parts of networks 1 and 2 increased with higher inattention scores. Network 1 exhibited high spatial similarity with the DMN and also included the insular and motor cortex, whereas network 2 resembled the fronto-parietal network. In contrast to network 4, these networks displayed average loadings on nearly all task aspects, indicating that these networks had an overall supportive role in executing the task, while being largely insensitive to reward.

Specifically, we observed inattention-related increases for seven functional connections within network 1, including increased functional connectivity of the FMC (blue and green) and PCC (blue) with the insular cortex (yellow) and large parts of the cerebellum (yellow). The FMC and PFC are key components of the DMN, which is, in contrast to task-positive networks, associated with self-referential cognitive processes that are typically inhibited during externally oriented, attention-demanding tasks (Buckner et al. 2008; Raichle et al. 2001). Our findings corroborate previous studies demonstrating decreased anti-correlation between task-positive networks in ADHD, including the insular cortex and cerebellum, and the DMN or, in other words, diminished suppression of the DMN (for review see Oldehinkel et al. 2013). As such, we interpret our findings according to the hypothesis that ADHD is associated with diminished suppression of the DMN, which disrupts ongoing cognition and behavior, leading to the inattentive behavior that is characteristic of ADHD (for review see Castellanos and Proal 2012). In addition, we observed that the average functional connectivity in a subnetwork (brown) within network 2, which showed high spatial overlap with the fronto-parietal network, increased with higher inattention scores. This finding supports previous studies relating reduced BOLD responses within the fronto-parietal network to impairments in cognitive control in ADHD (Hampshire and Sharp 2015; Smith et al. 2008; van Rooij et al. 2015) and R-fMRI studies that demonstrated reduced functional connectivity within the fronto-parietal network in ADHD (Cao et al. 2006; Cao et al. 2009).

Accordingly, one could speculate that our findings indicate that atypical reward processing in adolescents and adults with ADHD is not related to altered function in networks underlying reward processing, but results from secondary effects of alterations in more general task processing networks. The inattention-related increases in functional connectivity observed in the DMN and fronto-parietal network are consistent with this tentative hypothesis. That is, aberrant functional connectivity in general task-related networks might lead to altered attentional processes, affecting reward-sensitivity in participants with ADHD. Although many studies indicate that reward processing is aberrant in ADHD, the literature on the exact underlying mechanisms that lead to aberrant reward processing in ADHD is not settled at the behavioral nor at the neurobiological level (for reviews see Luman et al. 2005; Luman et al. 2010). For example, in their review Luman et al. (2005) discuss five theoretical models explaining altered reward sensitivity in ADHD and conclude that all these models contained insufficiencies in explaining the behavioral findings in their review. In addition, in task-based fMRI studies that investigated reward processing in ADHD, abnormal activations have also been reported in regions that are not typically associated with reward processing such as precuneus/PCC (Chantiluke

et al. 2014; Rubia et al. 2009), occipital cortex (von Rhein et al. 2015), and middle temporal and inferior frontal gyrus (Stoy et al. 2011), supporting our tentative hypothesis that altered reward processing in ADHD might result from secondary effects of alterations in more general task processing networks.

When further interpreting the absence of ADHD-related changes in functional connectivity of the primary reward regions in the context of the current literature, several factors need to be considered. First, the previous studies focused on children with ADHD (Costa Dias et al. 2012; Posner et al. 2013; Tomasi and Volkow 2012), whereas participants in our study were mostly adolescents and young adults with ADHD. As such, we investigated our sample at a different developmental stage compared to previous studies. Indeed, longitudinal structural MRI studies have provided evidence for diagnosis-specific developmental effects on the anatomy of regions in the brain (Castellanos et al. 2002; Shaw et al. 2007; Shaw et al. 2012). For example, delayed maturation of the PFC and caudate have been demonstrated in children with ADHD (Castellanos et al. 2002; Shaw et al. 2007). As such, abnormalities in the primary reward regions might be present in children with ADHD, whereas these abnormalities normalize over development and are not present anymore in (early) adulthood. Longitudinal R-fMRI studies are needed to determine whether the functional connectivity architecture of the networks underlying reward processing normalize over development in participants with ADHD.

Second, ADHD is characterized by large phenotypic heterogeneity, reflected by differences between subjects in ADHD subtype, symptom severity, and cognitive impairments (Coghill et al. 2014; Mostert et al. 2015; Nigg et al. 2005). This large phenotypic heterogeneity in ADHD might be related to a possible large heterogeneity in the underlying neurobiology. As such, not all participants with ADHD might display (similar) alterations in reward-related behavior and in functional connectivity of networks supporting reward processing. Indeed, in a recent study, Costa Dias and colleagues identified three distinct subgroups within typically developing children and children with ADHD by employing clustering to participant level whole-brain functional connectivity maps of a region corresponding to left NAcc (Costa Dias et al. 2015). All three subgroups displayed different connectivity patterns of the NAcc and differences in impulsivity. The existence of different subgroups based on NAcc connectivity might not only relate to the inconsistency of findings in previous R-fMRI studies in children with ADHD, but could also explain the absence of significant ADHD-related alterations in functional connectivity of the primary reward regions in this study. That is, classical case-control comparisons and dimensional analyses based on continuous symptom measures might not enable detection of ADHD-related effects on functional connectivity, when distinct subgroups exist that each has a distinct connectivity profile. Accordingly, disentangling subgroups within the ADHD and control population based on connectivity within the reward system holds potential for future research.

Finally, it has to be noted that our methodology differed from previous R-fMRI studies investigating the reward system in ADHD. Previous studies investigated functional connectivity of the reward system using the NAcc as seed region (Costa Dias et al. 2015; Costa Dias et al. 2012; Posner et al. 2013) or by using short and long-range functional connectivity density (Tomasi and Volkow 2012). In our study, we applied a principled, data-driven approach to obtain all networks involved in reward processing and subsequently investigated functional connectivity between subregions within these networks. As such, our approach entails a bottom-up and more holistic investigation of reward-related structures compared to investigations that target connectivity of a specific region or focus on a specific connectivity metric.

5. Conclusion

We did not replicate previous childhood findings of aberrant functional connectivity between key regions of the reward system in a large ADHD sample of adolescents and young adults. Yet, we did observe ADHD-related alterations in functional connectivity of areas in the DMN and fronto-parietal network, which support general task performance. Future work should aim to disentangle whether ADHD is primarily related to dysfunction of main task-supporting networks, rather than an outcome of disruptions in more specialized functional brain networks.

Funding

NeuroIMAGE is supported by NWO Large Investment grant 1750102007010, EU FP7 grant TACTICS (grant no. 278948), ZonMW Addiction: Risk Behaviour and Dependency Grant 60-60600-97-193, NWO Brain & Cognition: an Integrative Approach grant 433-09-242, and NWO National Initiative Brain & Cognition 056-13-015. Christian F. Beckmann is supported by the Netherlands Organisation for Scientific Research (NWO-Vidi 864-12-003) and received funding from the Wellcome Trust UK Strategic Award [098,369/Z/12/Z]. Barbara Franke's research is supported by grants from the Netherlands Organization for Scientific Research (NWO), i.e., the NWO Brain & Cognition Excellence Program (grant 433-09-229) and a Vici grant (grant 016-130-669). Her research also received funding from the European Community's Seventh Framework Programme (FP7/2007–2013) under grant agreements no. 602805 (Aggressotype) and no. 602450 (IMAGEMEND), and from the European Community's Horizon 2020 Programme (H2020/2014–2020) under grant agreements no. 643051 (MiND and no. 667302 (CoCA). In addition, her work is supported by a grant for the ENIGMA Consortium (grant number U54 EB020403) from the BD2K Initiative of a cross-NIH partnership. Maarten Mennes is supported by a Marie Curie International Incoming Fellowship under the European Union's Seventh Framework Programme (FP7/2007–2013), grant agreement no. 327340 (Brain Fingerprint). This work was further supported by National Institutes of Health grant R01MH62873 (Dr. Faraone) and grants from Radboudumc, University Medical Center Groningen, Accare, and Vrije Universiteit Amsterdam.

Conflict of interest

Jan K. Buitelaar has been a consultant to/member of advisory boards of and/or a speaker for Janssen-Cilag BV, Eli Lilly, Bristol-Myers Squibb, Schering Plough, UCB, Shire, Novartis, Roche, and Servier. He is not an employee of any of these companies, and not a stock shareholder of any of these companies. Barbara Franke has received an educational speaking fee from Merz. Pieter J. Hoekstra has received an unrestricted research grant from Shire and has been member of the advisory boards of Shire and Eli Lilly. Jaap Oosterlaan has received an unrestricted investigator initiated research grant from Shire Pharmaceuticals. All other authors reported no biomedical financial interests or conflicts of interest.

Appendix A. Supplementary data.

Supplementary data to this article can be found online at doi:10.1016/j.nicl.2016.10.006.

References

Bitsakou, P., Psychogiou, L., Thompson, M., Sonuga-Barke, E.J., 2009. Delay aversion in attention deficit/hyperactivity disorder: an empirical investigation of the broader phenotype. Neuropsychologia 47, 446–456.

Buckner, R.L., Andrews-Hanna, J.R., Schacter, D.L., 2008. The brain's default network: anatomy, function, and relevance to disease. Ann. N. Y. Acad. Sci. 1124, 1–38.

Cao, Q., Zang, Y., Sun, L., Sui, M., Long, X., Zou, Q., Wang, Y., 2006. Abnormal neural activity in children with attention deficit hyperactivity disorder: a resting-state functional magnetic resonance imaging study. Neuroreport 17, 1033–1036.

Cao, X., Cao, Q., Long, X., Sun, L., Sui, M., Zhu, C., Zuo, X., Zang, Y., Wang, Y., 2009. Abnormal resting-state functional connectivity patterns of the putamen in medication-naive children with attention deficit hyperactivity disorder. Brain Res. 1303, 195–206.

Castellanos, F.X., Proal, E., 2012. Large-scale brain systems in ADHD: beyond the prefrontal-striatal model. Trends Cogn. Sci. 16, 17–26.

Castellanos, F.X., Lee, P.P., Sharp, W., Jeffries, N.O., Greenstein, D.K., Clasen, L.S., Blumenthal, J.D., James, R.S., Ebens, C.L., Walter, J.M., Zijdenbos, A., Evans, A.C., Giedd, J.N., Rapoport, J.L., 2002. Developmental trajectories of brain volume abnormalities in children and adolescents with attention-deficit/hyperactivity disorder. JAMA 288, 1740–1748.

Chantiluke, K., Christakou, A., Murphy, C.M., Giampietro, V., Daly, E.M., Ecker, C., Brammer, M., Murphy, D.G., Rubia, K., 2014. Disorder-specific functional abnormalities during temporal discounting in youth with attention deficit hyperactivity disorder (ADHD), autism and comorbid ADHD and autism. Psychiatry Res. 223, 113–120.

Coghill, D.R., Seth, S., Matthews, K., 2014. A comprehensive assessment of memory, delay aversion, timing, inhibition, decision making and variability in attention deficit hyperactivity disorder: advancing beyond the three-pathway models. Psychol. Med. 44, 1989–2001.

Conners, C.K., Sitarenios, G., Parker, J.D., Epstein, J.N., 1998a. The revised Conners' Parent Rating Scale (CPRS-R): factor structure, reliability, and criterion validity. J. Abnorm. Child Psychol. 26, 257–268.

Conners, C.K., Sitarenios, G., Parker, J.D., Epstein, J.N., 1998b. Revision and restandardization of the Conners Teacher Rating Scale (CTRS-R): factor structure, reliability, and criterion validity. J. Abnorm. Child Psychol. 26, 279–291.

Costa Dias, T.G., Wilson, V.B., Bathula, D.R., Iyer, S.P., Mills, K.L., Thurlow, B.L., Stevens, C.A., Musser, E.D., Carpenter, S.D., Grayson, D.S., Mitchell, S.H., Nigg, J.T., Fair, D.A., 2012. Reward Circuit Connectivity Relates to Delay Discounting in Children with Attention-Deficit/Hyperactivity Disorder (Eur Neuropsychopharmacol).

Costa Dias, T.G., Iyer, S.P., Carpenter, S.D., Cary, R.P., Wilson, V.B., Mitchel, S.H., Nigg, J.T., Fair, D.A., 2015. Characterizing heterogeneity in children with and without ADHD based on reward system connectivity. Dev Cogn Neurosci 11, 155–174.

Di Martino, A., Scheres, A., Margulies, D.S., Kelly, A.M., Uddin, L.Q., Shehzad, Z., Biswal, B., Walters, J.R., Castellanos, F.X., Milham, M.P., 2008. Functional connectivity of human striatum: a resting state FMRI study. Cereb. Cortex 18, 2735–2747.

Faraone, S.V., Biederman, J., Mick, E., 2006. The age-dependent decline of attention deficit hyperactivity disorder: a meta-analysis of follow-up studies. Psychol. Med. 36, 159–165.

Greve, D.N., Fischl, B., 2009. Accurate and robust brain image alignment using boundary-based registration. NeuroImage 48, 63–72.

Groen, Y., Gaastra, G.F., Lewis-Evans, B., Tucha, O., 2013. Risky behavior in gambling tasks in individuals with ADHD–a systematic literature review. PLoS One 8, e74909.

Haber, S.N., Knutson, B., 2010. The reward circuit: linking primate anatomy and human imaging. Neuropsychopharmacology 35, 4–26.

Hampshire, A., Sharp, D.J., 2015. Contrasting network and modular perspectives on inhibitory control. Trends Cogn. Sci. 19, 445–452.

Hauser, T.U., Iannaccone, R., Ball, J., Mathys, C., Brandeis, D., Walitza, S., Brem, S., 2014. Role of the medial prefrontal cortex in impaired decision making in juvenile attention-deficit/hyperactivity disorder. JAMA Psychiatry 71, 1165–1173.

Jenkinson, M., Bannister, P., Brady, M., Smith, S., 2002. Improved optimization for the robust and accurate linear registration and motion correction of brain images. NeuroImage 17, 825–841.

Kaufman, J., Birmaher, B., Brent, D., Rao, U., Flynn, C., Moreci, P., Williamson, D., Ryan, N., 1997. Schedule for affective disorders and schizophrenia for school-age children-present and lifetime version (K-SADS-PL): initial reliability and validity data. J. Am. Acad. Child Adolesc. Psychiatry 36, 980–988.

Liu, X., Hairston, J., Schrier, M., Fan, J., 2011. Common and distinct networks underlying reward valence and processing stages: a meta-analysis of functional neuroimaging studies. Neurosci. Biobehav. Rev. 35, 1219–1236.

Luman, M., Oosterlaan, J., Sergeant, J.A., 2005. The impact of reinforcement contingencies on AD/HD: a review and theoretical appraisal. Clin. Psychol. Rev. 25, 183–213.

Luman, M., Tripp, G., Scheres, A., 2010. Identifying the neurobiology of altered reinforcement sensitivity in ADHD: a review and research agenda. Neurosci. Biobehav. Rev. 34, 744–754.

Marco, R., Miranda, A., Schlotz, W., Melia, A., Mulligan, A., Muller, U., Andreou, P., Butler, L., Christiansen, H., Gabriels, I., Medad, S., Albrecht, B., Uebel, H., Asherson, P., Banaschewski, T., Gill, M., Kuntsi, J., Mulas, F., Oades, R., Roeyers, H., Steinhausen, H.C., Rothenberger, A., Faraone, S.V., Sonuga-Barke, E.J., 2009. Delay and reward choice in ADHD: an experimental test of the role of delay aversion. Neuropsychology 23, 367–380.

Morel, A., 2007. Stereotactic Atlas of the Human Thalamus and Basal Ganglia. CRC Press.

Mostert, J.C., Onnink, A.M., Klein, M., Dammers, J., Harneit, A., Schulten, T., van Hulzen, K.J., Kan, C.C., Slaats-Willemse, D., Buitelaar, J.K., Franke, B., Hoogman, M., 2015. Cognitive heterogeneity in adult attention deficit/hyperactivity disorder: a systematic analysis of neuropsychological measurements. Eur. Neuropsychopharmacol. 25, 2062–2074.

Nigg, J.T., Willcutt, E.G., Doyle, A.E., Sonuga-Barke, E.J., 2005. Causal heterogeneity in attention-deficit/hyperactivity disorder: do we need neuropsychologically impaired subtypes? Biol. Psychiatry 57, 1224–1230.

Oldehinkel, M., Francx, W., Beckmann, C., Buitelaar, J., Mennes, M., 2013. Resting state FMRI research in child psychiatric disorders. Eur. Child Adolesc. Psychiatry 22, 757–770.

O'Reilly, J.X., Beckmann, C.F., Tomassini, V., Ramnani, N., Johansen-Berg, H., 2010. Distinct and overlapping functional zones in the cerebellum defined by resting state functional connectivity. Cereb. Cortex 20, 953–965.

Plichta, M.M., Scheres, A., 2014. Ventral-striatal responsiveness during reward anticipation in ADHD and its relation to trait impulsivity in the healthy population: a meta-analytic review of the fMRI literature. Neurosci. Biobehav. Rev. 38, 125–134.

Pollen, D.A., 1999. On the neural correlates of visual perception. Cereb. Cortex 9, 4–19.

Posner, J., Rauh, V., Gruber, A., Gat, I., Wang, Z., Peterson, B.S., 2013. Dissociable attentional and affective circuits in medication-naive children with attention-deficit/hyperactivity disorder. Psychiatry Res. 213, 24–30.

Pruim, R.H., Mennes, M., Buitelaar, J.K., Beckmann, C.F., 2015a. Evaluation of ICA-AROMA and alternative strategies for motion artifact removal in resting state fMRI. NeuroImage 112, 278–287.

Pruim, R.H., Mennes, M., van Rooij, D., Llera, A., Buitelaar, J.K., Beckmann, C.F., 2015b. ICA-AROMA: a robust ICA-based strategy for removing motion artifacts from fMRI data. NeuroImage 112, 267–277.

Raichle, M.E., MacLeod, A.M., Snyder, A.Z., Powers, W.J., Gusnard, D.A., Shulman, G.L., 2001. A default mode of brain function. Proc. Natl. Acad. Sci. U. S. A. 98, 676–682.

Rubia, K., Smith, A.B., Halari, R., Matsukura, F., Mohammad, M., Taylor, E., Brammer, M.J., 2009. Disorder-specific dissociation of orbitofrontal dysfunction in boys with pure conduct disorder during reward and ventrolateral prefrontal dysfunction in boys with pure ADHD during sustained attention. Am. J. Psychiatry 166, 83–94.

Scheres, A., Milham, M.P., Knutson, B., Castellanos, F.X., 2007. Ventral striatal hyporesponsiveness during reward anticipation in attention-deficit/hyperactivity disorder. Biol. Psychiatry 61, 720–724.

Shaw, P., Eckstrand, K., Sharp, W., Blumenthal, J., Lerch, J.P., Greenstein, D., Clasen, L., Evans, A., Giedd, J., Rapoport, J.L., 2007. Attention-deficit/hyperactivity disorder is characterized by a delay in cortical maturation. Proc. Natl. Acad. Sci. U. S. A. 104, 19649–19654.

Shaw, P., Malek, M., Watson, B., Sharp, W., Evans, A., Greenstein, D., 2012. Development of cortical surface area and gyrification in attention-deficit/hyperactivity disorder. Biol. Psychiatry 72, 191–197.

Smith, A.B., Taylor, E., Brammer, M., Halari, R., Rubia, K., 2008. Reduced activation in right lateral prefrontal cortex and anterior cingulate gyrus in medication-naive adolescents with attention deficit hyperactivity disorder during time discrimination. J. Child Psychol. Psychiatry 49, 977–985.

Smith, S.M., Beckmann, C.F., Andersson, J., Auerbach, E.J., Bijsterbosch, J., Douaud, G., Duff, E., Feinberg, D.A., Griffanti, L., Harms, M.P., Kelly, M., Laumann, T., Miller, K.L., Moeller, S., Petersen, S., Power, J., Salimi-Khorshidi, G., Snyder, A.Z., Vu, A.T., Woolrich, M.W., Xu, J., Yacoub, E., Ugurbil, K., Van Essen, D.C., Glasser, M.F., 2013. Resting-state fMRI in the human connectome project. NeuroImage 80, 144–168.

Sonuga-Barke, E.J., 2005. Causal models of attention-deficit/hyperactivity disorder: from common simple deficits to multiple developmental pathways. Biol. Psychiatry 57, 1231–1238.

Stoy, M., Schlagenhauf, F., Schlochtermeier, L., Wrase, J., Knutson, B., Lehmkuhl, U., Huss, M., Heinz, A., Strohle, A., 2011. Reward processing in male adults with childhood ADHD–a comparison between drug-naive and methylphenidate-treated subjects. Psychopharmacology 215, 467–481.

Tomasi, D., Volkow, N.D., 2012. Abnormal functional connectivity in children with attention-deficit/hyperactivity disorder. Biol. Psychiatry 71, 443–450.

Uebel, H., Albrecht, B., Asherson, P., Borger, N.A., Butler, L., Chen, W., Christiansen, H., Heise, A., Kuntsi, J., Schafer, U., Andreou, P., Manor, I., Marco, R., Miranda, A., Mulligan, A., Oades, R.D., van der Meere, J., Faraone, S.V., Rothenberger, A., Banaschewski, T., 2010. Performance variability, impulsivity errors and the impact of incentives as gender-independent endophenotypes for ADHD. J. Child Psychol. Psychiatry 51, 210–218.

van Rooij, D., Hoekstra, P.J., Mennes, M., von Rhein, D., Thissen, A.J., Heslenfeld, D., Zwiers, M.P., Faraone, S.V., Oosterlaan, J., Franke, B., 2015. Distinguishing adolescents with ADHD from their unaffected siblings and healthy comparison subjects by neural activation patterns during response inhibition. Am. J. Psychiatr. 172, 674–683.

von Rhein, D., Mennes, M., van Ewijk, H., Groenman, A.P., Zwiers, M.P., Oosterlaan, J., Heslenfeld, D., Franke, B., Hoekstra, P.J., Faraone, S.V., 2014. The NeuroIMAGE study: a prospective phenotypic, cognitive, genetic and MRI study in children with attention-deficit/hyperactivity disorder. Design and descriptives. Eur. Child Adolesc. Psychiatry 24, 265–281.

von Rhein, D., Cools, R., Zwiers, M.P., van der Schaaf, M., Franke, B., Luman, M., Oosterlaan, J., Heslenfeld, D.J., Hoekstra, P.J., Hartman, C.A., 2015. Increased neural responses to reward in adolescents and young adults with attention-deficit/hyperactivity disorder and their unaffected siblings. J. Am. Acad. Child Adolesc. Psychiatry 54, 394–402.

Winkler, A.M., Ridgway, G.R., Webster, M.A., Smith, S.M., Nichols, T.E., 2014. Permutation inference for the general linear model. NeuroImage 92, 381–397.

Zhang, D., Snyder, A.Z., Shimony, J.S., Fox, M.D., Raichle, M.E., 2010. Noninvasive functional and structural connectivity mapping of the human thalamocortical system. Cereb. Cortex 20, 1187–1194.